UNIVERSIDAD SAN FRANCISCO DE QUITO USFQ

Colegio de Ciencias e Ingenierías

Delays in Actuation Channel and Transmitter: Implications for Control System Performance

Jimmy Sebastián Alarcón Calle

Ingeniería en Electrónica y Automatización

Trabajo de fin de carrera presentado como requisito
para la obtención del título de
Ingeniero en Electrónica

Quito, 17 de mayo de 2024

UNIVERSIDAD SAN FRANCISCO DE QUITO USFQ

Colegio de Ciencias e Ingenierías

HOJA DE CALIFICACIÓN
DE TRABAJO DE FIN DE CARRERA

Delays in Actuation Channel and Transmitter: Implications for Control System Performance

Jimmy Sebastián Alarcón Calle

Nombre del profesor, Título académico **Oscar Camacho, PhD**

Quito, 17 de mayo de 2024

© DERECHOS DE AUTOR

Nombres y apellidos: Jimmy Sebastián Alarcón Calle

Código: 00215922

Cédula de identidad: 1708521495

Lugar y fecha: Quito, 17 de mayo de 2024

ACLARACIÓN PARA PUBLICACIÓN

UNPUBLISHED DOCUMENT

RESUMEN

En los procesos industriales, los retardos pueden surgir de diversas fuentes y comprender sus efectos es crucial para un control y una optimización eficaces. Este artículo investiga los efectos de los retardos en los canales de los actuadores y transmisores sobre el rendimiento del sistema de control. Además, evalúa, a partir de las consideraciones de Bode, la relación entre los dos retardos y qué estrategia de control podría ser más apropiada. Para ello, aplicamos un proceso matemático para obtener sus respectivas ecuaciones de magnitud y fase para comprender su comportamiento en los diagramas de Bode.

Palabras clave: retardo de tiempo, sistemas de control, análisis, rendimiento, diagramas de Bode.

ABSTRACT

In industrial processes, delays can arise from various sources and understanding their effects is crucial to effective control and optimization. This paper investigates the effects of delays in actuator channels and transmitters on the performance of the control system. In addition, it evaluates from Bode's considerations the relationship between the two delays and their relationship and which control strategy could be more appropriate. For this purpose, we apply a mathematical process to obtain its respective magnitude and phase equations to understand its behavior on Bode diagrams.

Index Terms: time delay, control systems, analysis, performance, Bode diagrams.

CONTENIDO

ÍNDICE DE TABLAS

ÍNDICE DE FIGURAS

1. INTRODUCTION

In numerous practical engineering systems, time delays are common, whether in the state, in the control input, or in measurements. The time delay occurs when a mass or energy is transported within a medium. This delay plays a significant role in complex fields of communication and information technologies, such as the stabilization of networked control systems and high-speed communication networks. Often, this time delay can lead to instability in many cases [Fridman, 2014]

Transmission systems, chemical processes, metallurgical processes, hydraulic and pneumatic systems, power systems, biological systems, the environment, and ecosystems are examples of time delayed systems [Camacho and Leiva, 2020]. Therefore, time delays can occur in industrial processes for various reasons, and understanding the existence of time delays is essential for effective control and optimization [Smith, 2002]. They can significantly affect closed-loop control performance, especially with substantial dead time. Problems related to increased dead time include decreased cross- over frequencies and critical gains, making the controller more noise-sensitive. Furthermore, the controller takes longer to take corrective actions, and the system's transient behavior becomes slower, increasing the risk of instability [Mejia et al., 2022, Espin et al., 2022].

Delays in sensor measurements can affect the accuracy of feedback control. Suppose there are significant delays between when a process variable changes and when the sensor detects the change. In that case, the control system may react too late, leading to deviations from the desired setpoint; the risk of oscillations can appear since delays in sensor measurements can lead to control system oscillations as the controller tries to compensate for perceived errors caused by the delayed feedback. In addition, delays in actuator response times can slow the system's ability to adjust process variables in response to control commands. This can affect the system's ability to maintain setpoints and respond to disturbances promptly. The previous considerations affect stability. Excessive delays in actuator response can lead to control instability, especially in systems with fast-changing dynamics.

Communication delay or control delay between the central controller and remote field devices can introduce delays in control loops. These delays can affect the system's ability to maintain process stability and performance. It should be noted that delays in data exchange between control system parts, such as the supervisory control level and field devices, can affect coordination and decision-making. This problem is typical in distributed control systems.

Delays can impact the precision of model forecasts, particularly in systems characterized by intricate dynamics or long transport durations; if the mathematical models employed for control and optimization fail to consider delays precisely, the effectiveness of control strategies may be compromised, resulting in less-than-optimal performance.

As mentioned in previous paragraphs, delays present multifaceted challenges that significantly influence the effectiveness of control and optimization. Therefore, this research explores the repercussions of delays within actuator channels and transmitters on control system performance. In addition, it evaluates from Bode's considerations the relationship between these delays and stability and makes some considerations on its impact on control systems.

This paper is organized as follows. Section 2 presents the fundamentals explaining the general delay categories. Section 3 shows the stability of Bode diagrams, including concepts. Section 4 presents the experimental results. Conclusions are shown in Section 5.

2. MAIN BODY

2.1. General Delay Categories and Feedback Control

The challenges posed by time delays in control systems can be broadly categorized into two main areas. The first category pertains to delays in sensors or measurement devices, where the controller receives outdated information about the process behavior. The second category involves delays in the actuation channels, where the control action cannot be applied in a timely manner, thus reducing the effectiveness of compensation for disturbances and other factors.

2.1.1. Delays in Actuation Channel

Actuation channels are the pathways through which control commands are sent from a controller to actuators (e.g., motors, valves) to manipulate a system. Delays in actuator channels can arise from various sources, including communication delays, signal processing delays, and physical response times of actuators. Delays in actuation channels can vary widely depending on the specific system. In some applications, these delays can be minimal, in milliseconds or microseconds, especially in systems where real-time control is critical. Delays may occurring more complex systems or in slower actuators in seconds or minutes.

2.1.2. Delays in Transmitter

Transmitters send information or signals, including control commands or sensor data, from one location to another. Delays in transmitters can be caused by signal propagation time, data processing time, and communication protocol overhead. Transmitter delays can also vary widely. In wired communication systems, delays are typically very short, often measured in microseconds to milliseconds. In wireless communication systems, delays can be slightly longer due to signal propagation through the air. Depending on factors such as distance and the kind of controlled variable, they can range from milliseconds to a few minutes or hours.

2.1.3. Feedback Control of Delayed Systems

As is known, in the Laplace domain, a pure delay can be represented as e−t0s where t0 represents the delay or the dead time.

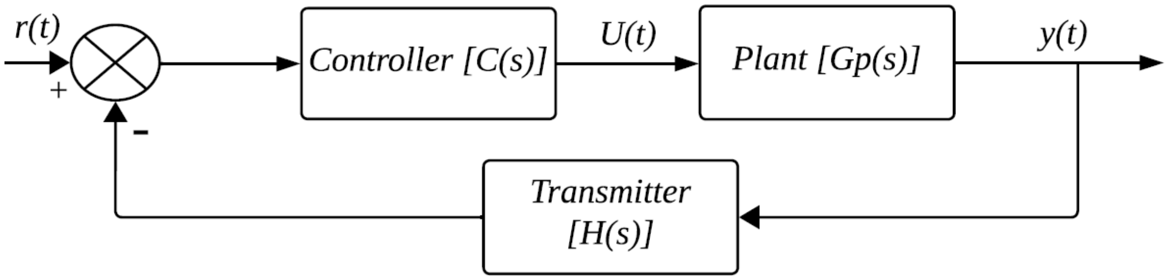

Figure 1: Simplified diagram of a feedback system

In this work, we consider the fact that the plant and transmitter can be approximated by first order plus deadtime (FOPDT). This model represents many industrial processes [Smith, 2002] and is obtained using the reaction curve procedure [Smith, 2002].

$$G_m(s) = \frac{Ke^{-t_0 s}}{\tau s + 1} \tag{1}$$

where K is a static gain, t_0 is a time delay, and τ is a time constant.

- Delay in output (delay in state):

Consequently, the first type of delay affecting the output or the state can be termed a delay in the output or the state (as depicted in Figure 1). The closed-loop transfer function is as follows:

$$\frac{X(s)}{R(s)} = G(s) = \frac{C(s)G_m(s)}{1 + C(s)G_m(s)e^{-t_{01}s}} \tag{2}$$

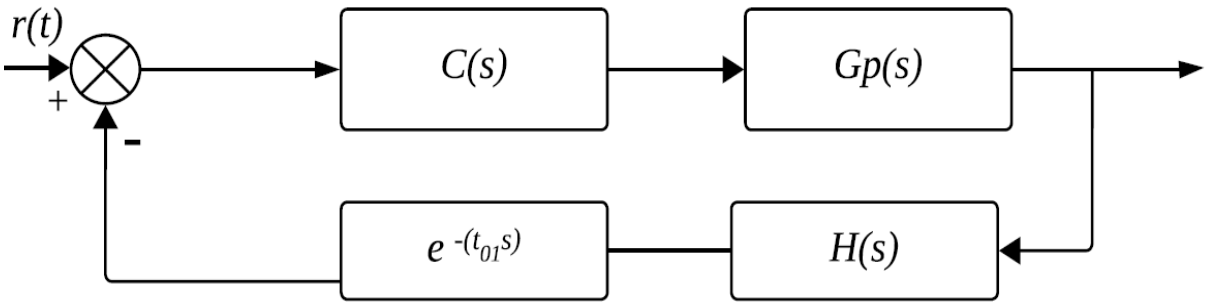

Figure 2: Simplified diagram of a delay in output system

- Delay in input (delay in control):

In contrast, the second type, which affects the input or the control, is called a delay in the input or the control (as illustrated in Figure 2), and its closed-loop transfer function is as presented:

$$\frac{X(s)}{R(s)} = G(s) = \frac{C(s)e^{-t_{02}s}G_m(s)}{1 + C(s)e^{-t_{02}s}G_m} \tag{3}$$

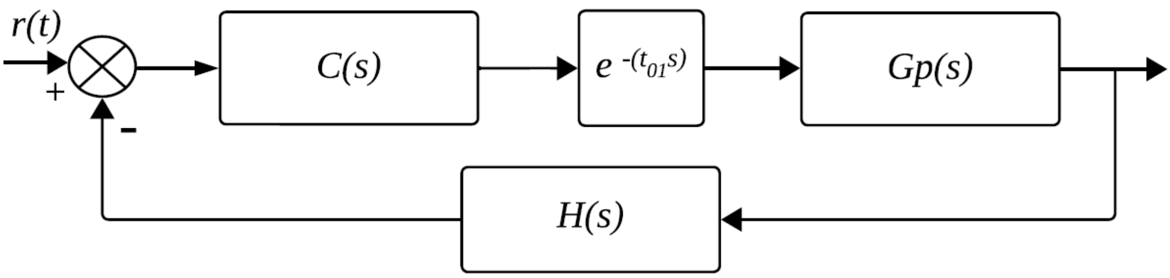

Figure 3: Simplified diagram of a delay in input system

In both cases, the presence of loop delays typically imposes stringent constraints on the achievable feedback performance, as appears in the closed-loop transfer function of the system [Camacho and Leiva, 2020]

- Delay in output plus Delay in input simultaneously:

A third case can be considered if both delays are present simultaneously (Figure 1c). The relationship between delay in actuation channels and transmitters in a control system can vary widely. There is no fixed ratio as it depends on the factors of the system. In some cases, delays in both aspects are comparable when fast actuators and sensors are used. In other situations, one delay may dominate; for example, actuators might be slower than fast transmitting sensors.

Actuation and transmitter delays can have different time constants due to physical and communication factors; the transfer function for this case is as follows.

$$\frac{X(s)}{R(s)} = G(s) = \frac{C(s)e^{-t_{02}s}G_m(s)}{1 + C(s)e^{-t_{02}s}G_m(s)e^{-t_{01}s}} \tag{4}$$

The previous equation can be rewritten as follows:

$$\frac{X(s)}{R(s)} = G(s) = \frac{C(s)e^{-t_{02}s}G_m(s)}{1 + C(s)G_m(s)e^{-(t_{01}+t_{02})s}} \tag{5}$$

In this case, several results can be obtained depending on the values of the two delays and their relationship.

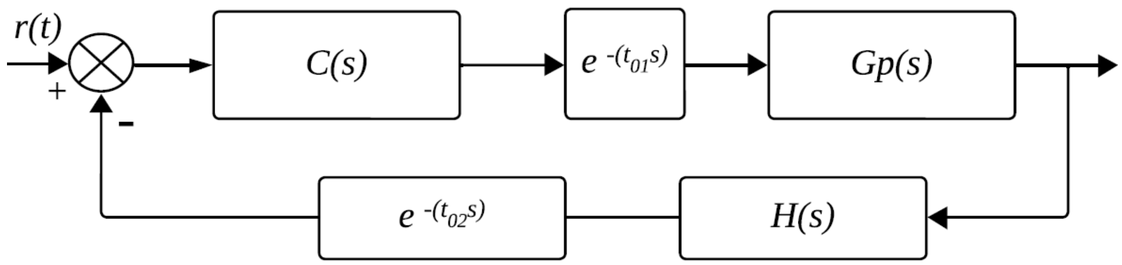

Figure 4: Simplified diagram of a delay in output and delay in input system

3. CONTROL LOOP STABILITY USING BODE DIAGRAMS:

This section presents stability analysis using bode diagrams [Smith, 2002]. The idea behind the study isto see the effect of the controllability relationship on the gain and phase margins.

3.1. Definitions

Previously, we distinguished some concepts.

- **Controllability relationship:** The controllability ratio ($t0/\tau$) is associated with the difficulty level in controlling a process. It is also known as normalized dead time or normalized time delay [Obando et al., 2023]. Generally speaking, processes with small ($t0/\tau$) are simple to regulate, and as a system gets bigger ($t0/\tau$), it is harder to control.
- **Gain Margin:** Measures the stability of a control system and represents the amount by which the system's gain can be increased before it becomes unstable. It is typically expressed in decibels (dB) and indicates the amount of amplification that can be applied to the system without causing oscillations or instability [Ogata and Yang, 2002].
- **Phase Margin:** Quantifies how much additional phase shift can be applied in the system's feedback loop before it becomes unstable. The phase margin is usually expressed in degrees and represents the difference between the phase shift of the system at the critical frequency (where the gain crossover occurs) and -180 degrees [Ogata and Yang, 2002].

3.2. Systems with delay: Gain and phase calculations

Consider a general FOPDT model.

$$G(s) = \frac{Ke^{-t_0 s}}{\tau s + 1} \tag{6}$$

With $K = 1$

Changing s = jw, the previous equation can be rewritten as

$$G(s) = \frac{e^{-jwt_0}}{\tau wj + 1} \tag{7}$$

The logarithmic magnitude is

$$20log \mid G(jw) \mid = 20log \mid e^{-jwt_0} \mid + 20log \mid \frac{1}{\tau jw + 1} \mid \tag{8}$$

$$20log \mid G(jw) \mid = 0 + 20log \mid \frac{1}{\tau jw + 1} \mid \tag{9}$$

As can be seen, the delay does not contribute to the magnitude.

The phase angle of the transfer function is given by

$$\angle\, G(jw) \;= -\angle\, (-wt_0) - tan^{-1}(w\tau) \tag{10}$$

We change this ratio from 0 to 2 to show how the controllability relationship ($t0/\tau$) affects stability. The following figures are obtained using Matlab for the Bode analysis.

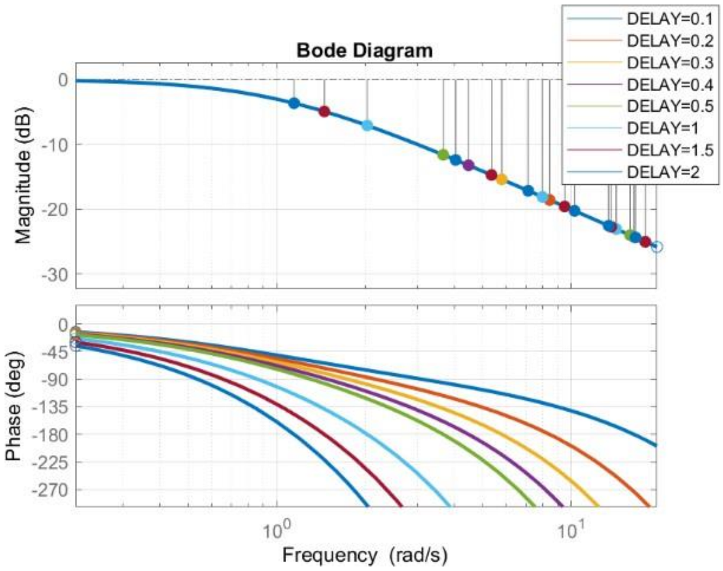

Figure 5: Bode Plot changing t0/τ from 0 to 2

Completing Figure 5 requires a thorough understanding of the calculations for the gain and phase margins. The phase margin is derived by first pinpointing the frequency at which the system's gain hits 0 decibels on the Bode diagram, then referring to the corresponding phase angle on the same chart; the next step is to subtract the phase angle from -180 degrees to get the phase margin. The Gain Margin signifies the degree to which the system's gain can be increased before it becomes unstable and is measured in decibels. Navigating the Bode diagram involves finding the frequency where the phase crosses -180°, a common sign of phase crossover in negative feedback systems; at this point, the gain value is noted, usually directly from the Bode plot. The gain margin is calculated by subtracting this gain value from 0 dB, which offers crucial information on the stability of the system under different gain scenarios; the interested reader can revise [Smith, 2002]. These values show how changes influence the gain andphase margins in t0/τ.

In summary, when t0 increases, the phase decreases, affecting the stability of the process since *MG* decreases, as shown in Fig. 5.

With Figure 5, we now obtain the first table to understand the behavior of the system; this can help us better predict the stability range.

Table 1: Gain Margin variation for controllability changes

K	t_0/τ	MG (dB)
1	0.1	24.3
1	0.2	18.6
1	0.3	15.4
1	0.4	13.2
1	0.5	11.6
1	1	7.09
1	1.5	4.92
1	2	3.64

then, with the values of the Margin Gain (MG), we need to obtain the values of *KM* with the following equation:

$$20log_{10}(K_M) = MG \tag{11}$$

Given that *MG* is a measure of the amount by which the system's gain can be increased before it becomes unstable, we calculate the maximum KM, see Table 6, for the system. This is the esult of using Equation 11. To tune the controller, we divide the maximum values by two.

Table 2: Critical controller gain

t_0/τ	K_M
0.1	16.405
0.2	8.511
0.3	5.888
0.4	4.570
0.5	3.801
1	2.262
1.5	1.761
2	1.520

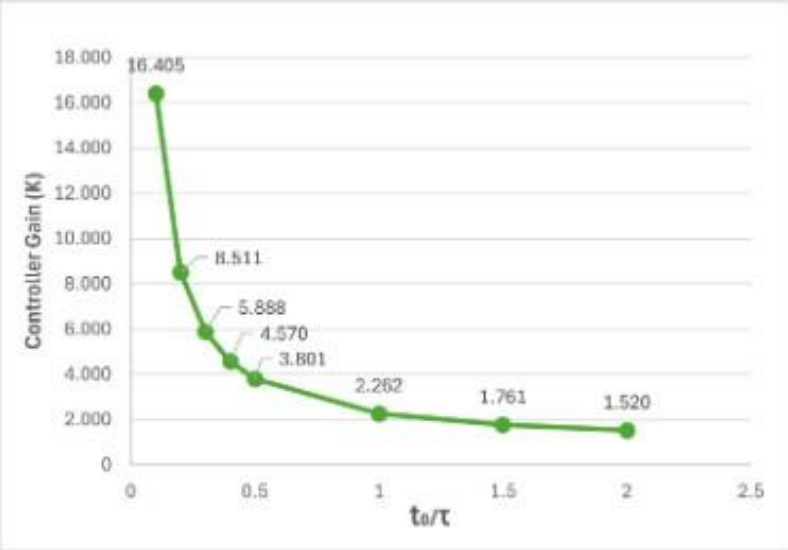

Figure 6: Gain variations vs t0/T

The previous graph shows that when (t0/τ) is greater than one, the gain decreases, representing a difficult-to-control process with a dominant time delay.

Time response simulations were performed using a P controller with the proportional controller gain tuned considering the maximum gain divided by two, as shown in the next figures.

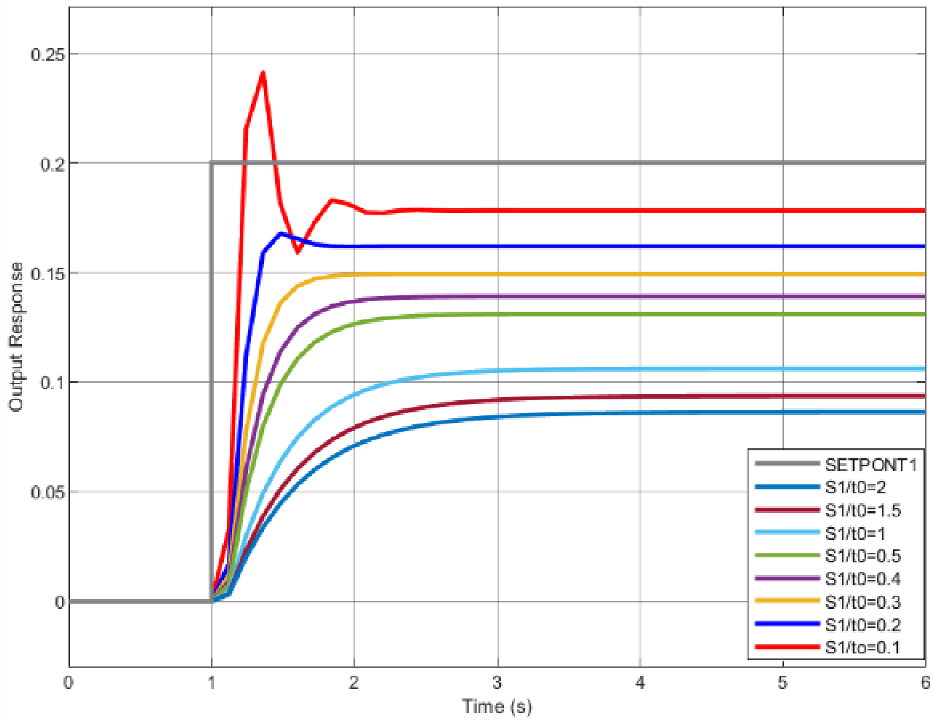

Figure 7: Process response for several t0/T values

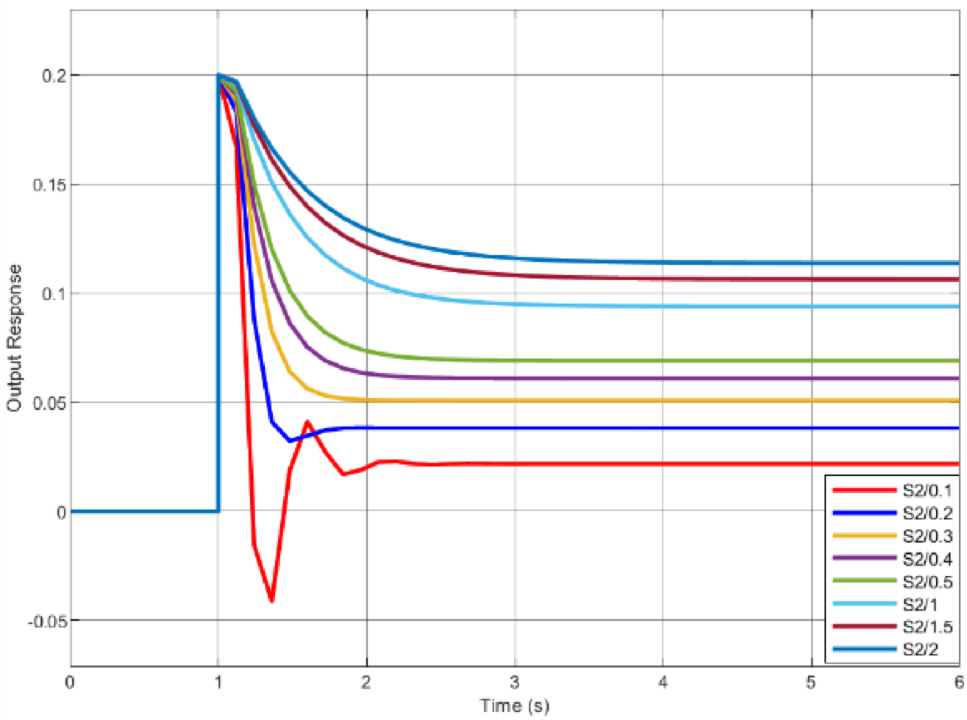

Figure 8: Controller Response for several t0/T values

4. RESULTS AND DISCUSSION

In this section, two experiments are done. The first using simulation and thesecond using TCLAB.

4.1. Simulation example- Dryer system

Identification of the system:

The following transfer functions that represent a dryer system [Smith, 2002] are presented as follows:

$$G_v(s) = \frac{0.016}{3s+1} \tag{12}$$

$$G_p(s) = \frac{50}{30s+1} \tag{13}$$

$$H(s) = \frac{1}{10s+1} \tag{14}$$

They represent the valve transfer function, the process transfer function, and the transmitter transfer function, respectively; as is observed, the process does not have a delay in time. We are adding the three cases presented before and doing a PID controller (Bode Analysis) to see the effect of the different delays on the process performance.

4.2 Simulation system analysis:

For this section, we need to follow a procedure, these are obtained based on smith's formulas [Smith, 2002].

First, we calculated *k*, that is equal to the difference of the transmitter output over the input signal. The parameters are calculated to obtain the FOPDT model of the plant with the following expressions [Smith, 2005]:

$$K = \Delta y / \Delta x \tag{15}$$

$$\tau = 1.5\left(t_{63.2\%} - t_{28.3\%}\right) \tag{16}$$

$$t_0 = t_{63.2\%} - \tau \tag{17}$$

For the system:

$$K = \frac{\Delta y}{\Delta x} = \frac{0.4}{0.5} = 0.8 \tag{18}$$

Using times t_1 and t_2, we apply the following equation to derive the time constant, τ:

$$\tau = 1.5(t_2 - t_1) = 1.5(44.646 - 22.25) = 33.594 \tag{19}$$

Lastly, to determine the time delay, t_0, we utilize the following equation:

$$t_0 = t_2 - \tau = 44.646 - 33.594 = 11.052 \tag{20}$$

Now, we can present the first-order plus delay time with the values of K, τ, and t_0. (FOPDT) approximation:

$$G_m(s) = \frac{0.8}{33.594s + 1} e^{-11.052} \tag{21}$$

To verify the obtained model, the process response output of the obtained model and the system is compared.

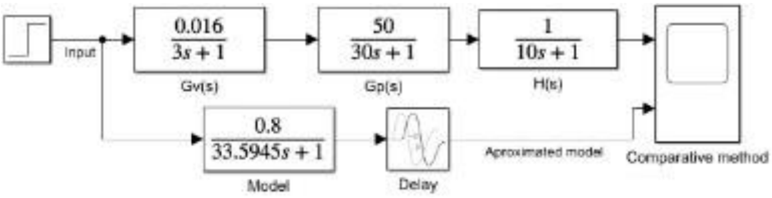

Figure 9: Diagram of comparative of the model vs the system

As observed in the results from figure 10, this method is highly efficient forreplicating the system, thereby achieving the modeling of an FOPDT.

Table 3: Terms for PID

Term	*Value*
Kp	1.8997
Ki	0.02976
Kd	5.526

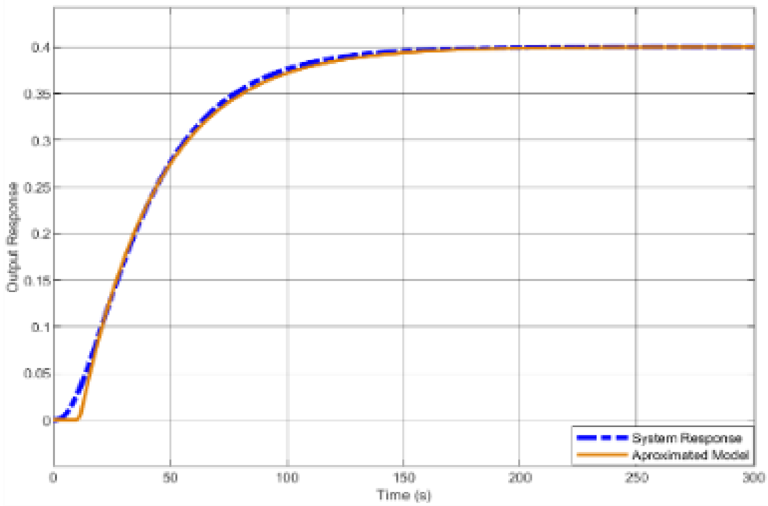

Figure 10: comparative of the model vs the system

To implement PID tuning using Dahlin's equations, we utilize the previously calculated parameters for the proportional, integral, and derivative terms from table 3.

Using the obtained values, it is proposed to apply this to the following cases.

4.3. With no delays

For this case the objective is to analyze the response of the system without delays because we need to compare the changes with respect to each case.

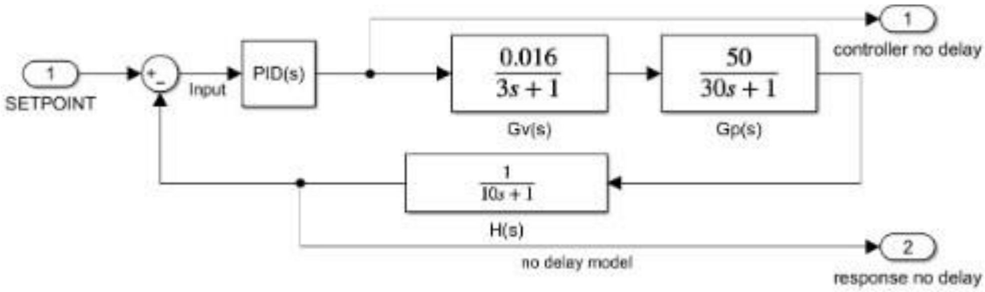

Figure 11: Diagram with no delays system

4.4. Delays in channel:

Based on the arguments in Table 3. Now we add a PID and a delay in the system's channel, and this is one of the most common cases we already see in practice.

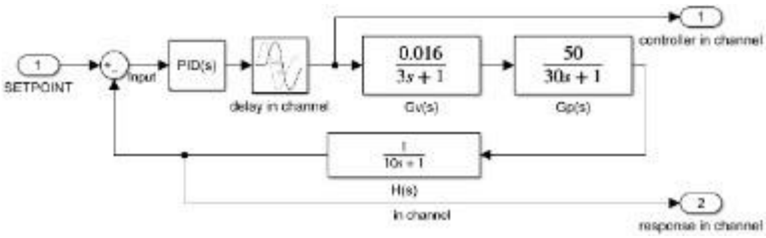

Figure 12: diagram with delay in the channel

4.5. Delays in transmitter:

We changed the diagram to add a delay in the transmitter; this means the output of the system.

4.6. Delays in transmitter and channel

Finally, we add both previously reviewed delays to analyze the process response, which is the most significant for this investigation.

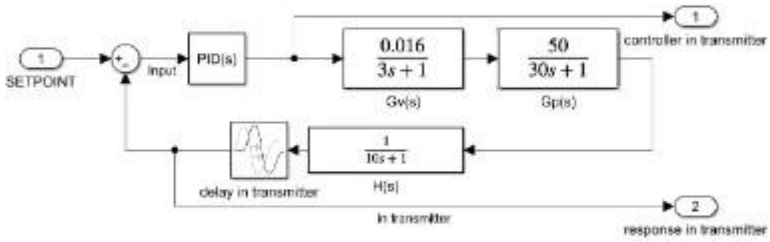

Figure 13: diagram with delay in the transmitter

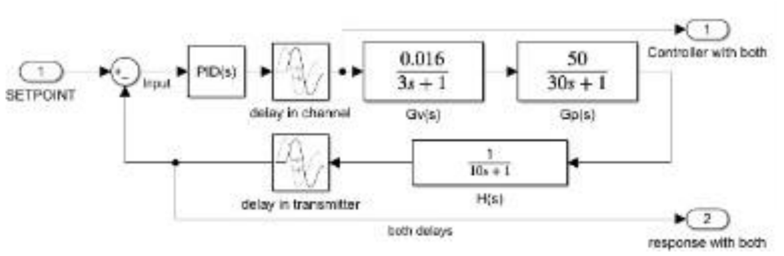

Figure 14: diagram with delays in transmitter and channel

With this diagram, we can obtain the result that the system produces when there is a presence of delay in both the input and output of the system.

4.7. Results with the simulations:

Then we simulated all this cases to see the process response:

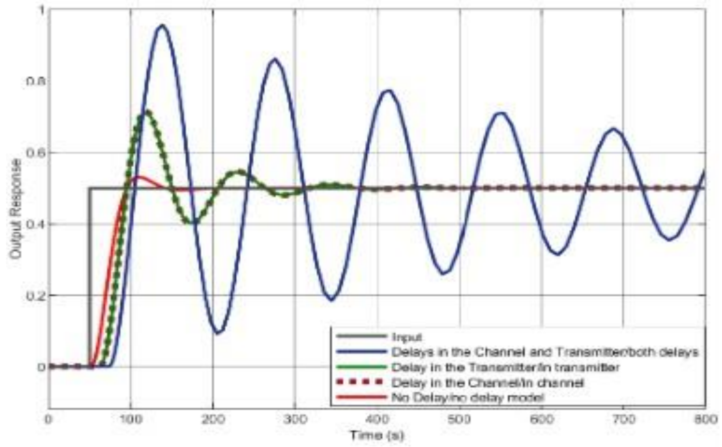

Figure 15: process response for all the cases

Figure 15 shows that the process response to the input delay is similar to the output delay. When both delays occur, the output response becomes more oscillatory, aligning with the analysis in section 2 when considering characteristic equations 2, 3, and 4.

Now, the controller action depicted in figure 18 exhibits a sharp response due to the derivative term.

To maintain the three obtained components of the controller, adjustments are needed; decreasing the derivative component or employing a pi controller are potential solutions. Analyzing the process responses, both input and output delays produce similar effects, despite the transmitter delay starting earlier.

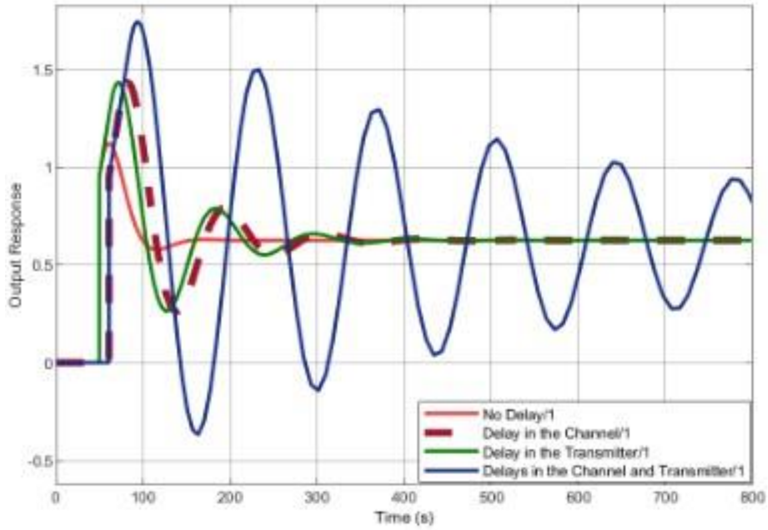

Figure 16. Controller response for all the cases

Compared to the channel delay in the controller action. It´s worth noting that the obtained delay is 11.052, meaning the initial value doubles for both input and output delays.

5. TCLAB EXPERIMENTATION

To experiment with this, the TCLAB (temperature controller LAB) will be employed, a device used for academic purposes to test control schemes. Initially, a process identification will be conducted to determine parameters and tune, followed by the implementation of a PI controller due to the temperature sensor generating high levels of noise, which wouldn't be adequately observed with a pid controller, across the four different cases.

5.1. Tclab model:

Firstly, we must follow the steps used in the previous simulation; therefore, we will begin by conducting a test to identify the response curve of the tclab to the changes in temperature applied. For this purpose, we will apply the following diagram: as can be observed, there is set of signals that will determine when the temperature of the device increases. this will progressively occur from the ambient temperature of approximately 23 °C, and then every 1000 seconds, it will add 20 degrees consecutively until reaching 100 degrees.

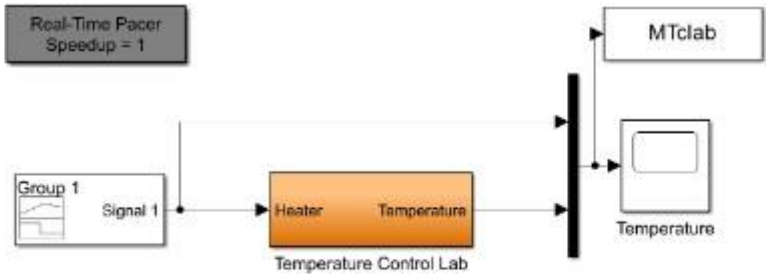

Figure 17. Diagram for obtain the response of the TClab

With the obtained graph, we proceed, using the method revised previously, to measure the parameters k, t0, and tau the obtained data is located in table 4:

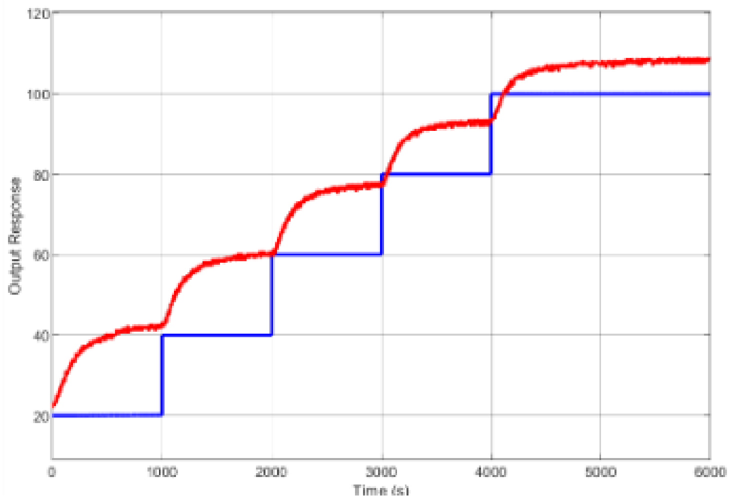

Figure 18: Response of the TClab

Table 4: Parameter Modeling Data

K	t_0	τ
0.969	31.678	210
0.904	32.021	172.8
0.831	25.973	166.944
0.831	22.683	174.951

Once this is done, we proceed to calculate the average values of each parameter, as shown in Table 5.

Table 5: Average: Parameter modeling Data

$Term$	$Value$
K	0.88375
T_0	28.08875
τ	174.951

With these values, we can now present the First-Order Plus Delay Time.(FOPDT) approximation of the Tclab.

$$G_m(s) = \frac{0.88375}{174.951s + 1} e^{-28.08875} \tag{22}$$

5.2.Comparative of the model with TClab:

To verify the obtained model, a comparison of the process response output is conducted between the obtained model and the TClab.

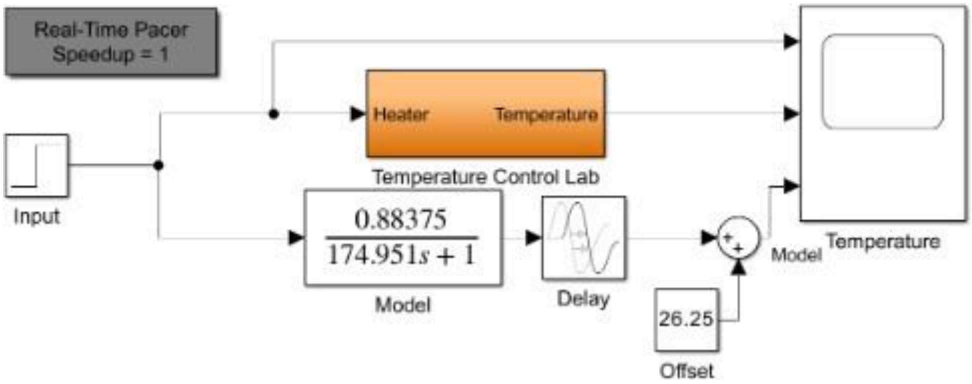

Figure 19: Diagram for obtain responses between TClab and model.

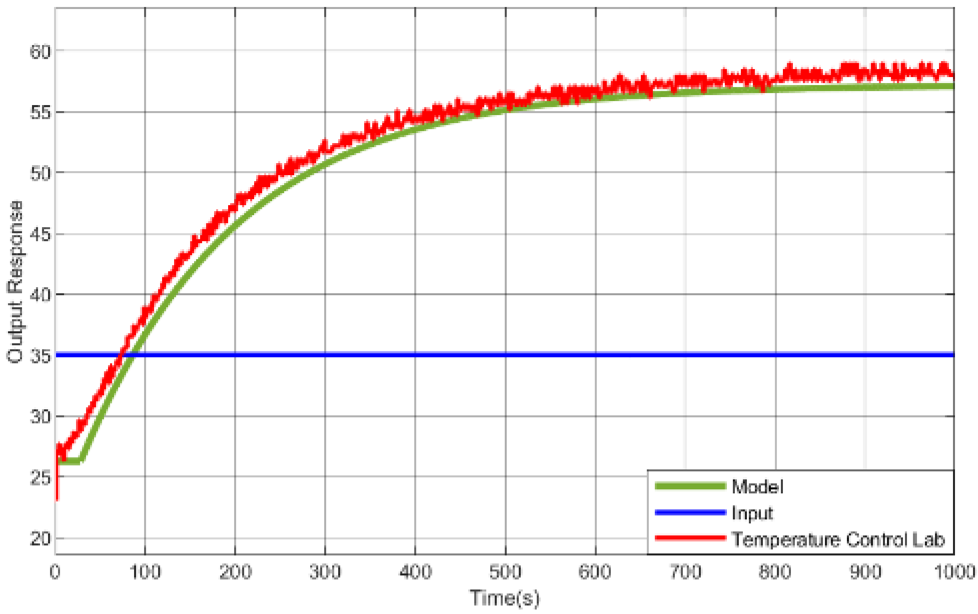

Figure 20: Comparison of responses between TClab and model

Through this comparative method, it can be affirmed that the analysis of the model has been successful, as the curves exhibit very similar responses. It should be noted that in processes where temperature is considered, the output points (offset) will always differ, therefore, it is recommended for the user to keep them as close as possible.

5.3. Cases of delay with TCLab:

Now, in order to implement PID tuning using Dahlin's equations, we employ the previously calculated parameters for the proportional, integral, and derivative terms from Table 6.

Table 6: Terms for PID

$Term$	$Value$
Kp	3.524
Ki	0.005715
Kd	14.044

Now, the analysis of the three previously reviewed cases will be conducted, for which we present each of their diagrams and illustrate the basis of their variations according to each case.

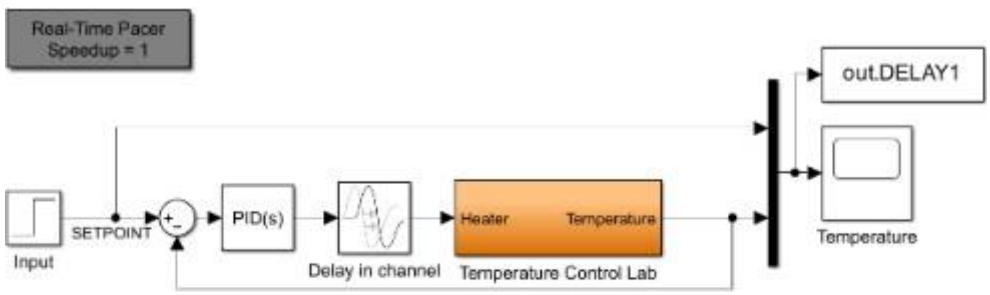

Figure 21: Diagram with delays in channel of TClab

5.4. Delay in Channel with TClab:

It is pertinent to mention that the cases will be analyzed for a temperature change from 20 to 35 °C.

5.5. Delay in Transmitter with TCLab:

It should also be noted that, through the MATLAB application, certain requirements must be met for the TClab device to function, primarily the controller authorized by Arduino to establish communication between the device and the computer.

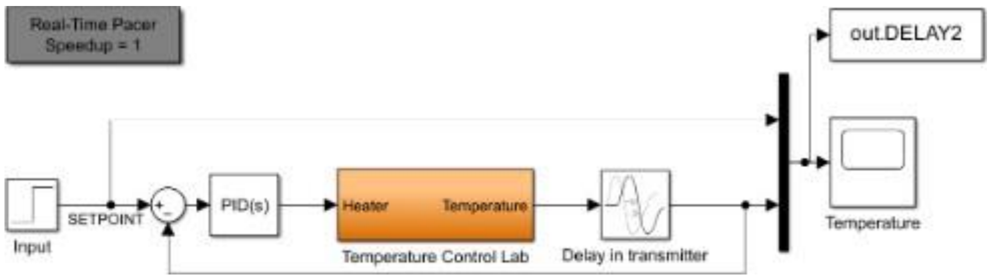

Figure 22: Diagram with delays in transmitter of TClab

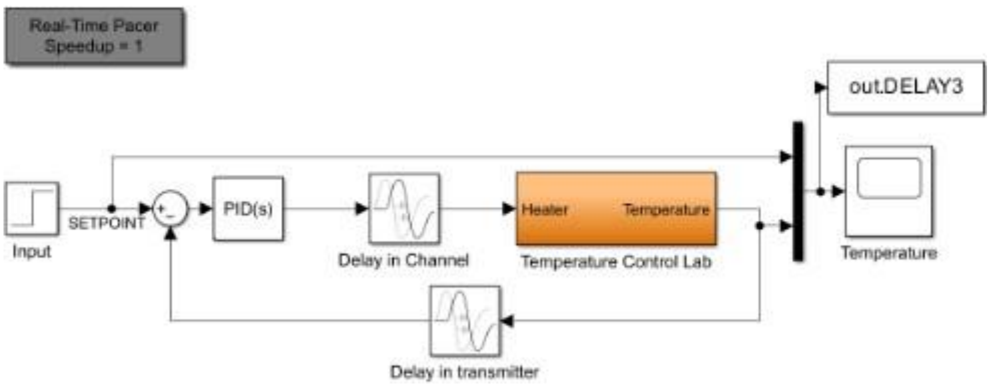

Figure 23: Diagram with delays in transmitter and channel of TClab

5.6. Delays in Channel and Transmitter with TClab:

As we observed, each case reflects the necessary changes to position the delay in the channel and the transmitter in the corresponding location.

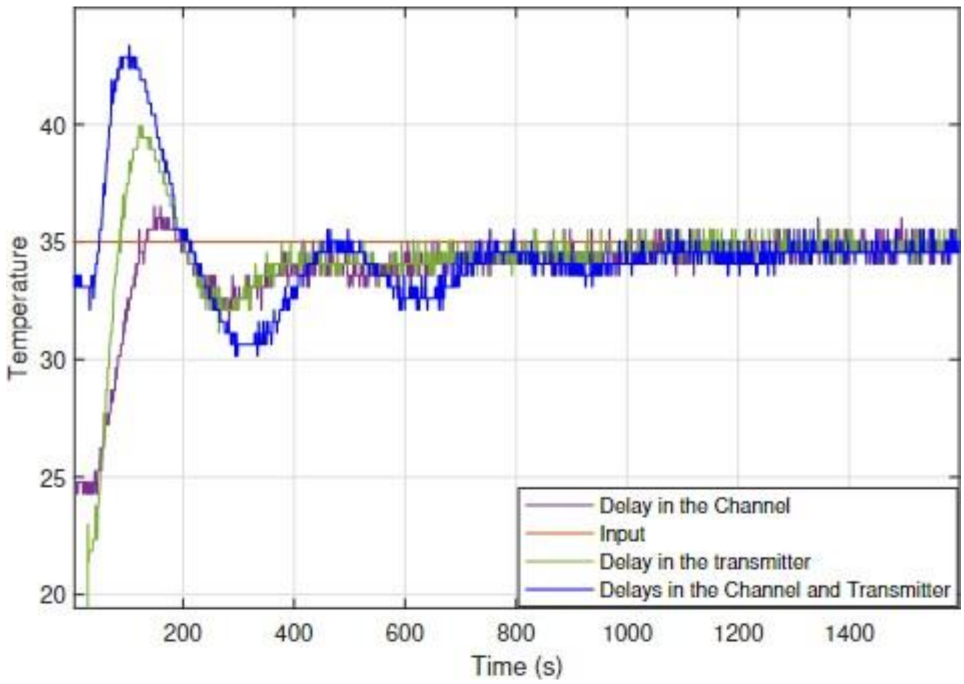

Figure 24: Comparison of the responses obtained from each case with TClab

5.7. Results with TClab:

Finally, we can observe each process response obtained from the TClab device. They are very similar to the responses obtained previously with the simulation model. Their main characteristic is that they maintain the relationship of having different starting points due to the delay with which they begin. For instance, in the case where the delay is in the transmitter, control begins later, causing the temperature to rise slightly higher compared to a simple delay in the channel. Therefore, in case three it can be clearly observed that this control process is very delayed and not suitable for temperature-related tasks, as it tends to be highly oscillatory, which could cause damage to the devices.

6. CONCLUSIONS

In summary, this work investigated the complex issues caused by delays in actuator channels and transmitters, highlighting their significant influence on the effectiveness of control and optimization procedures. Using Bode's observations, the study clarifies the complex relationship between these delays and system stability, providing insightful reflections on their repercussions for control systems. Through an exhaustive assessment, this research not only emphasizes the vital necessity of addressing delays in control systems but also imparts a detailed understanding of their subtle impacts, thus setting the stage for im- proved efficiency and dependability in forthcoming control system designs and executions.

Based on all the results obtained, it is suggested to conduct a study that analyzes this process using the Smith predictor method and a cascade method. This will allow for a more detailed diagnosis and exploration of control optimization options.

7. REFERENCES

Camacho, O. and Leiva, H. (2020). Impulsive semi-linear heat equation with delay in control and in state. Asian Journal of Control, 22(3):1075–1089.

Espin, J., Castrillon, F., Leiva, H., and Camacho, O. (2022). A modified smith predictor based–sliding mode control approach for integrating processes with dead time. Alexandria Engineering Journal, 61(12):10119–10137.

Fridman, E. (2014). Introduction to time-delay systems: Analysis and control. Springer.

Mejia, C., Salazar, E., and Camacho, O. (2022). A comparative experimental evaluation of various smith predictor approaches for a thermal process with large dead time. Alexandria Engineering Journal, 61(12):9377–9394.

Obando, C., Rojas, R., Ulloa, F., and Camacho, O. (2023). Dual-mode based sliding mode control approach for nonlinear chemical processes. ACS omega, 8(10):9511–9525.

Ogata, K. and Yang, Y. (2002). Modern control engineering, volume 5. Prentice hall India.

Smith, C. A. (2002). Automated continuous process control. John Wiley & Sons.

Smith, C. A. and Corripio, A. B. (2005). Principles and practices of automatic process control. John wiley & sons

8. ANEXOS

Anexo A: Diagrama para respuesta de simulación

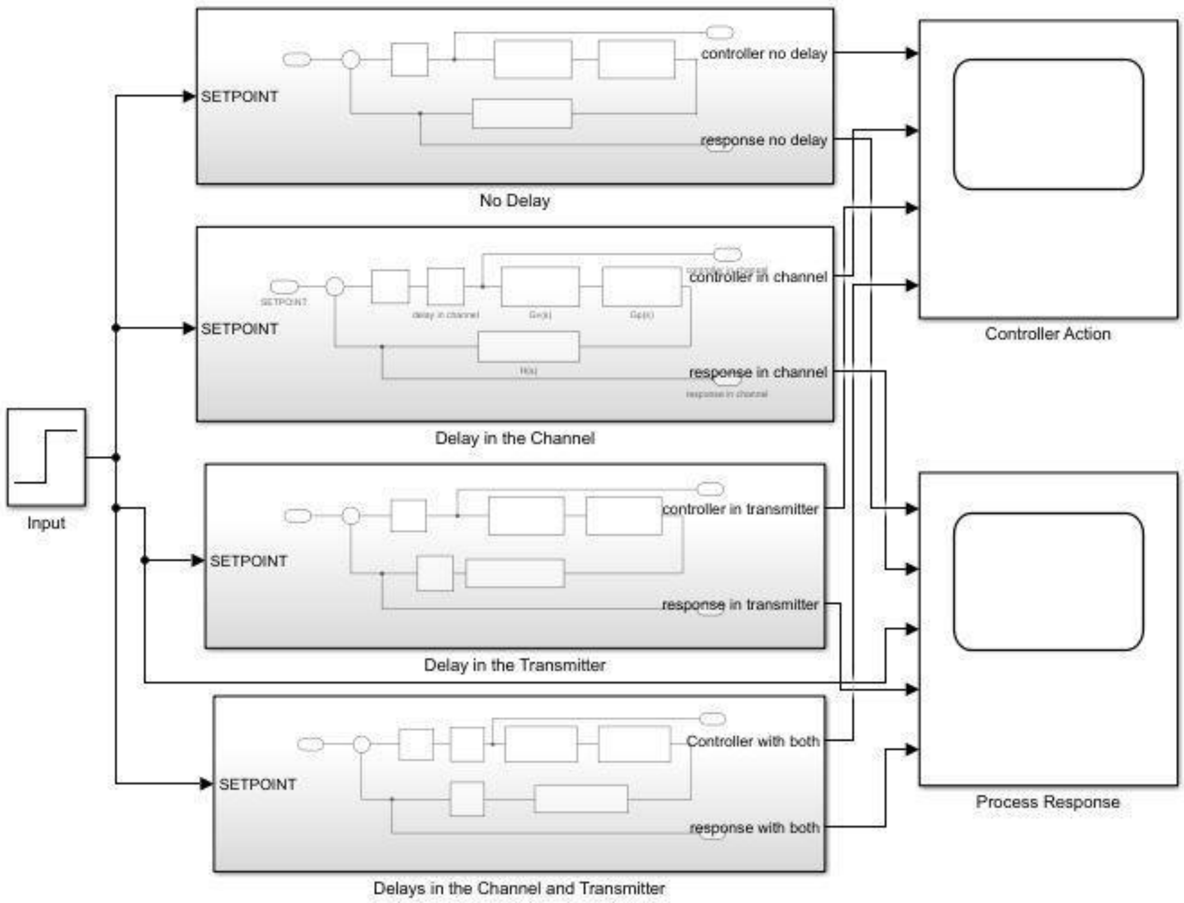

Anexo B: Diagrama respuesta de controlador P.

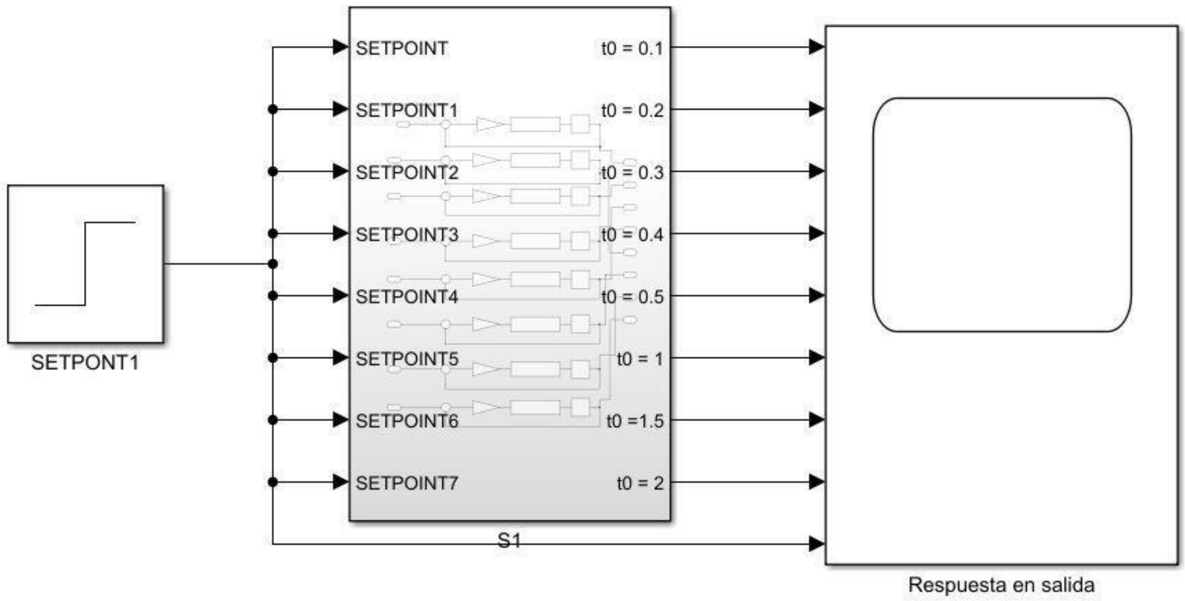

Anexo C: Diagrama para acción de control de controlador P